A Reconfigurable Aperture Antenna Based on Switched Links Between Electrically Small Metallic Patches

Lon N. Pringle, Paul H. Harms, *Member, IEEE*, Stephen P. Blalock, Gregory N. Kiesel, Eric J. Kuster, Paul G. Friederich, *Member, IEEE*, Ronald J. Prado, *Member, IEEE*, John M. Morris, and Glenn S. Smith, *Fellow, IEEE*

***Abstract*—A reconfigurable aperture (RECAP) antenna is described in which a planar array of electrically small, metallic patches are interconnected by switches. The antenna can be reconfigured to meet different performance goals by changing the switches that are open and closed. The switch configuration for a particular goal is determined using an optimizer, such as the genetic algorithm. First, the basic concept for the RECAP antenna is verified by comparing theoretical results with measurements for configurations in which the switches are simply wires connecting the patches. Next, details are given for a prototype antenna in which field-effect transistor based electronic switches are used with optical control. Theoretical results for the prototype antenna are then compared with measurements for cases in which electronic reconfiguration is used to change the bandwidth of operation or steer the pattern of the antenna. Finally, an overview of alternate switch/control strategies, some of which were tested, is given along with suggestions for improving the next generation of this antenna.**

***Index Terms*—Adaptive antenna, reconfigurable aperture.**

I. Introduction

WITH THE advances made in electronics, particularly reduction in size, it is now possible to employ many systems for communication, sensing, etc., in a single platform. These systems are linked to the "outside world" through antennas. When one antenna is allocated to each system, the platform quickly becomes littered with antennas. One way to alleviate this problem is to provide a single antenna that can be used for multiple systems. For example, an antenna can be designed to have a wide operational bandwidth so that it can be used for several communication channels. Another approach is to make the antenna *reconfigurable*. In the reconfigurable antenna, the structure of the antenna can be changed, for example, by changing the state of switches, to optimize the performance of the antenna for application in different systems.

Several approaches have been proposed for implementing the reconfigurable antenna. Most of these approaches make use of either electronic or electromechanical switches. The former includes switches based on the PIN diode or the field-effect transistor (FET), while the latter includes simple relays and a number of different types of microelectromechanical system (MEMS) switches. In some designs, the switches are used to change the length of an antenna element, such as a dipole or a slot, and, thereby, shift the frequency of operation (resonant point) [1]–[7]. Other designs involve structures with multiple layers. Each layer may be an array of antennas optimized to radiate in a particular frequency range or an image plane intended to reflect within a particular frequency range [8], [9]. The switches are then used to change which layer is operative. Other approaches make use of diodes with electronically variable capacitance (varactors) instead of switches. The diodes are incorporated into reflecting surfaces, and the variable capacitance is used to tune or steer the beam of an adjacent antenna [10], [11]. In another novel approach, plasma regions with fairly high electrical conductivity are temporarily created on a silicon substrate [12]. These regions define the antenna structure, and they can be changed to create different antennas.

In this paper, we describe the reconfigurable aperture (RECAP) antenna developed at the Georgia Tech Research Institute (GTRI) [13]–[16]. In Section II, the architecture for the antenna is described, and results from theoretical simulations [analysis with the finite-difference time-domain (FDTD) method] and measurements are presented that validate the basic concept. In Section III, the construction of the prototype antenna is described including the details for an FET-based electronic switch with its optically coupled control system. Results for the prototype antenna (theoretical simulations and measurements) are presented in Section IV. This includes cases where electronic reconfiguration is used to change the bandwidth of operation or steer the pattern of the antenna. In Section V, there is a brief discussion of alternative switch/control strategies for the antenna, some of which were tested during the program. This paper ends with a brief conclusion in Section VI.

II. Overview of the Architecture for the RECAP Antenna

Fig. 1 shows the basic architecture for the GTRI reconfigurable aperture antenna. A thin dielectric substrate supports an array of square, metallic patches. The patches are electrically small, that is, $l/\lambda_o << 1$, where l is the side length of the patch

Manuscript received January 28, 2003; revised May 9, 2003. This work was supported in part by the Defense Advanced Research Projects Agency (DARPA) under Contract DAAB07-99-C-K530.

L. N. Pringle, P. H. Harms, S. P. Blalock, G. N. Kiesel, E. J. Kuster, P. G. Friederich, R. J. Prado, and J. M. Morris are with the Georgia Institute of Technology Research Institute, Atlanta, GA 30332 USA (e-mail: lon.pringle@gtri.gatech.edu).

G. S. Smith is with the School of Electrical and Computer Engineering, Georgia Institute of Technology, Atlanta, GA 30332-0250 USA (e-mail: glenn.smith@ece.gatech.edu).

Digital Object Identifier 10.1109/TAP.2004.825648

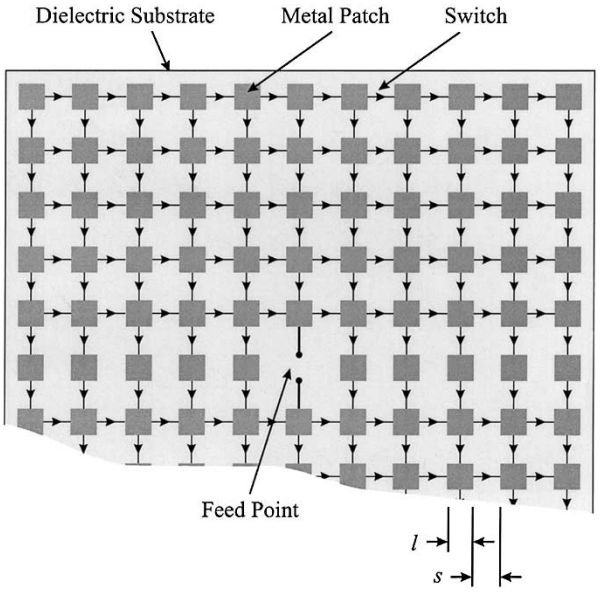

Fig. 1. Schematic drawing for the RECAP antenna architecture (dipole form).

and λ_o is the free space wavelength at the operating frequency. It is important to recognize that these elements are not conventional microstrip patch antennas. Each patch is connected to the surrounding patches by switched links, indicated by the arrows in the figure. Each switch may be open or closed depending upon the design requirements. There is a single feed point (pair of terminals) located at the center of the antenna.

For all of the antennas discussed in this paper, the aperture is formed from a printed circuit board 22.5×22 cm in size, with the patches etched from the copper cladding on one side of the board. The spacing between the patches is equal to the side length of a patch: $l = s = 1.0$ cm; see Fig. 1. There are a total of 120 patches and 208 switches on the board. The frequency of operation is within the range $0.85\ \text{GHz} \leq f \leq 1.45\ \text{GHz}$, thus $0.028 \leq l/\lambda_o \leq 0.048$. All of the antennas to be described in this paper have mirror symmetry about the horizontal line through the feed point. Note that this symmetry includes the states of the switches, i.e., open or closed. Thus, these antennas can be analyzed/measured in the "dipole form" shown in Fig. 1 or in the "monopole form" shown in Fig. 2.

Fig. 2 shows the experimental setup used for all of the measurements reported in this paper. The half-plane version of the RECAP antenna is mounted vertically on a rotatable disc centered in a large metallic image plane (6×6 m). The antenna is fed from below the image plane by a coaxial line (characteristic impedance $Z_c = 50\,\Omega$). The center conductor of the coaxial line is connected to the bottom patch in the center column of the RECAP antenna. A calibrated TEM horn antenna is located at a distance $r = 2$ m from the antenna. The scattering parameters for the two-port network formed by the RECAP antenna and the TEM horn are measured with a network analyzer and are used to determine the absolute gain for the RECAP antenna [17]. The horizontal field pattern ($|\vec{E}_\varphi|$ versus θ) for the RECAP antenna is obtained by rotating the disc/antenna while recording the output signal from the horn.

The procedure for designing a configuration for the RECAP antenna is based on a rigorous electromagnetic simulation of

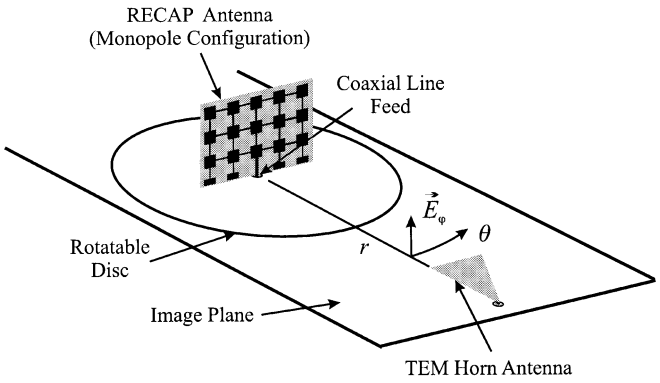

Fig. 2. Arrangement used for making measurements on the RECAP antenna (monopole form).

the antenna using the FDTD method [18]. First, a goal is established for the antenna, such as maximum gain over a particular bandwidth. Then, the FDTD simulation is run in conjunction with an optimizer, which for the work presented in this paper is one based on the genetic algorithm [19]. The optimizer attempts to determine the configuration for the switches (which switches should be open and which switches should be closed) that best meets the specified goal.[1]

To validate the design procedure, tests were first performed on RECAP antennas with "hard-wired" switches that were gaps either closed by a wire soldered in place or left open. The dielectric substrate was 1.7-mm-thick FR4 circuit board with the following measured electrical properties: $\varepsilon_r' = 4.27, \varepsilon_r'' = 0.07, \mu = \mu_o$. The goal for these designs was that the *realized gain* (the gain including mismatch) of the RECAP antenna should equal or exceed the *directivity* of a uniform sheet of vertically directed current of the same size.

Fig. 3(a) shows the switch configuration for a broadband, bidirectional, broadside design for the frequency range $0.85\ \text{GHz} \leq f \leq 1.25\ \text{GHz}$ (bandwidth of 38%). Notice that this configuration has right–left symmetry. All of the broadside designs to be discussed are constrained to have this symmetry. Fig. 4(a) shows the realized gain versus frequency; the dashed line is the aforementioned goal, the solid line is the FDTD simulation, and the line with the solid dots is the measured result.[2] The simulated and measured realized gains are in good agreement over the specified bandwidth, with a maximum difference of about 1 dB. The realized gain for the design is about 0.5–1.5 dB below the goal. A portion of this difference can be attributed to the mismatch at the feed of the RECAP antenna. In Fig. 4(b), the factor $(1 - |S_{11}|^2)$, which accounts for the loss in gain due to mismatch, is shown as a function of the frequency. Within the design bandwidth, it is within the range 0.0 to -1.5 dB. Fig. 5 shows the horizontal field pattern at the center frequency $f = 1.05$ GHz.[3] The shapes of the

[1]Taking into account the symmetry of the array, there are $2^{104} \approx 2 \times 10^{31}$ possible configurations for the switches, so with the capabilities of current computers, it is impossible to simulate all of the possible configurations and select the configuration with the optimum performance.

[2]In all of the FDTD simulations reported in the paper, cubical Yee cells were used with a side length of 2.5 mm.

[3]For all of the results to be presented, the realized gain is for the RECAP antenna in the dipole configuration.

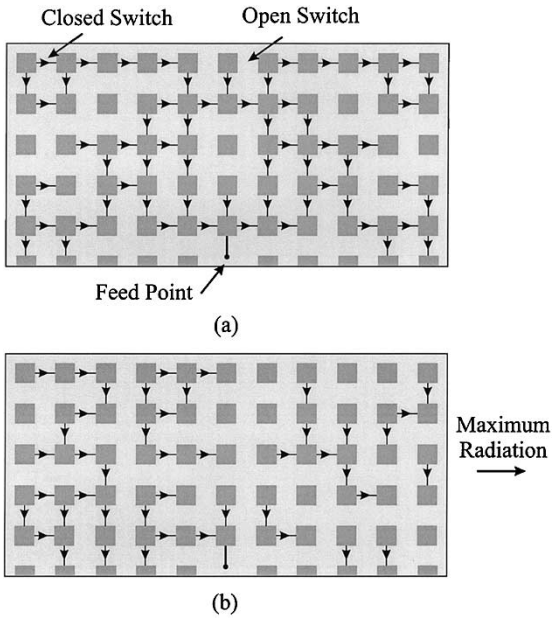

Fig. 3. Schematic drawing for the RECAP antenna (monopole form) showing which switches are open and closed when wires are used for closed switches. (a) Broadband, bidirectional, broadside design. (b) Narrow-band, unidirectional, endfire design.

simulated and measured field patterns are nearly the same; both are normalized to have a maximum of 0 dB. Note that the heavy line at the center of the field pattern indicates the orientation of the dielectric substrate for the RECAP antenna.

Fig. 3(b) shows the switch configuration for a narrow-band, unidirectional, end-fire design for the frequency range 1.0 GHz $\leq f \leq$ 1.1 GHz (bandwidth of 9.5%). Notice that this configuration does not have right–left symmetry and is quite different from the broadside design shown in Fig. 3(a). The goal is again that the realized gain of the RECAP antenna should equal or exceed the directivity of a uniform sheet of current; only now the current is phased to produce end-fire radiation. Fig. 6(a) shows the realized gain versus frequency. The nomenclature for the curves is the same as in the earlier example. Again, the simulated and measured realized gains are in good agreement over the specified bandwidth, with a maximum difference of about 1 dB. The realized gain for the design is about 1.0–2.0 dB below the goal, and as before a portion of this difference can be attributed to the mismatch at the feed of the RECAP antenna. In Fig. 6(b), the factor $(1-|S_{11}|^2)$, which accounts for the loss in gain due to mismatch, is shown as a function of the frequency. Within the design bandwidth, it is within the range 0.0 to -0.8 dB. Fig. 7 shows the horizontal field pattern at the center frequency $f = 1.05$ GHz. The shapes of the simulated and measured field patterns are nearly the same, and both are clearly end-fire patterns.

In typical configurations, like those discussed in this paper, about 30–60% of the switches in the RECAP antenna are closed. One might expect that an examination of the states of the switches (which ones are open and which ones are closed) for a particular design would give some insight into how the genetic algorithm optimized the antenna for the particular goal. For example, for the unidirectional, end-fire design described

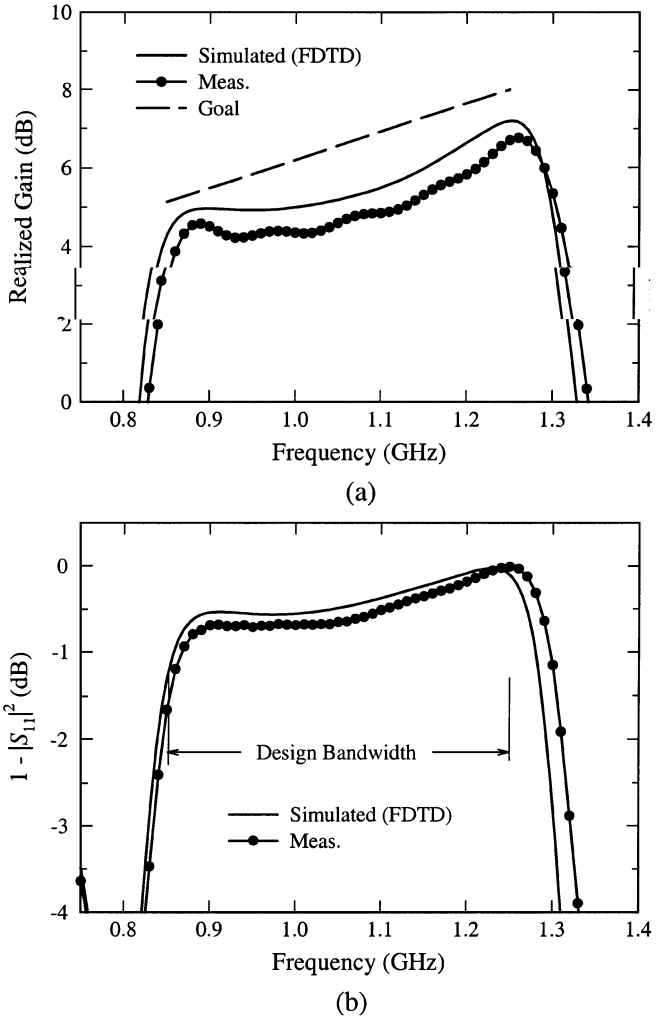

Fig. 4. Comparison of simulated results with measurements for a broadband, bidirectional, broadside design with wires for closed switches. (a) Realized gain versus frequency. (b) Decrease in gain due to mismatch: $1-|S_{11}|^2$.

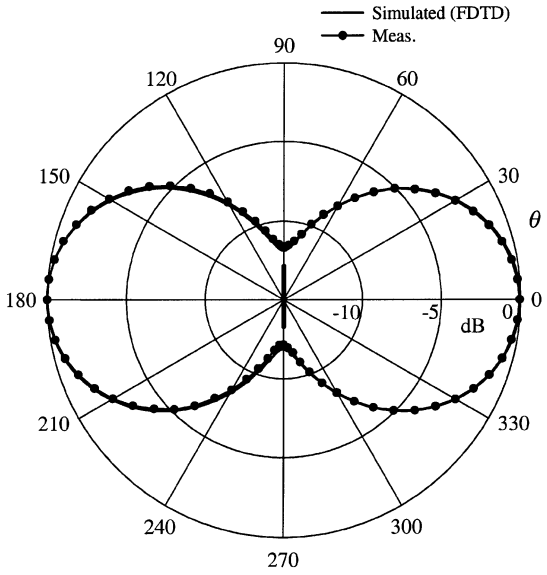

Fig. 5. Comparison of simulated results with measurements for a broadband, bidirectional, broadside design with wires for closed switches. Horizontal field pattern at the center frequency $f = 1.05$ GHz. Both patterns are normalized to 0 dB.

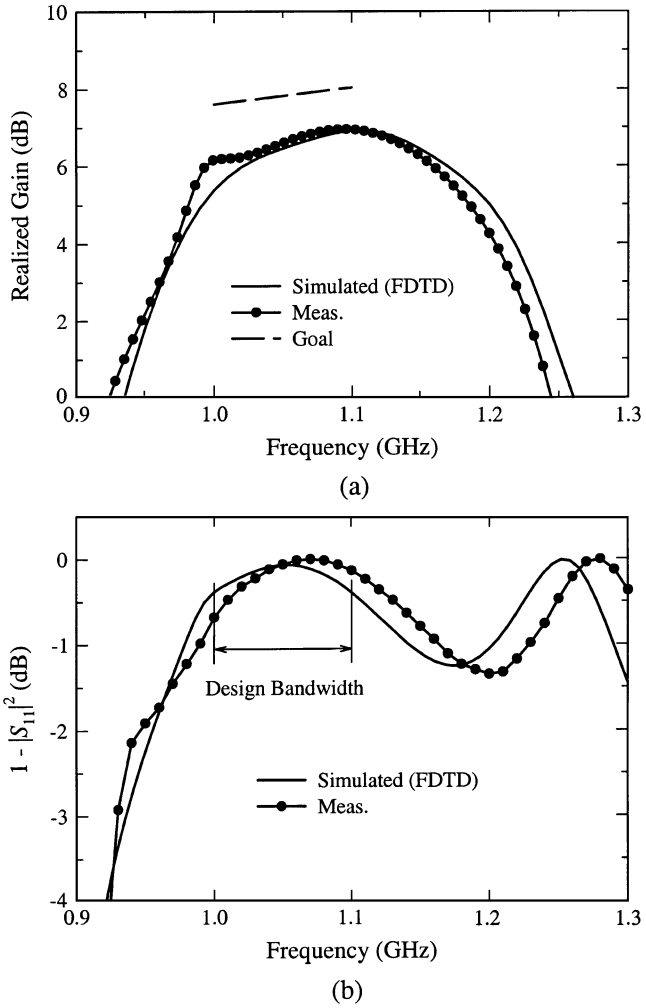

Fig. 6. Comparison of simulated results with measurements for a narrow-band, unidirectional, end-fire design with wires for closed switches. (a) Realized gain versus frequency. (b) Decrease in gain due to mismatch: $1-|S_{11}|^2$.

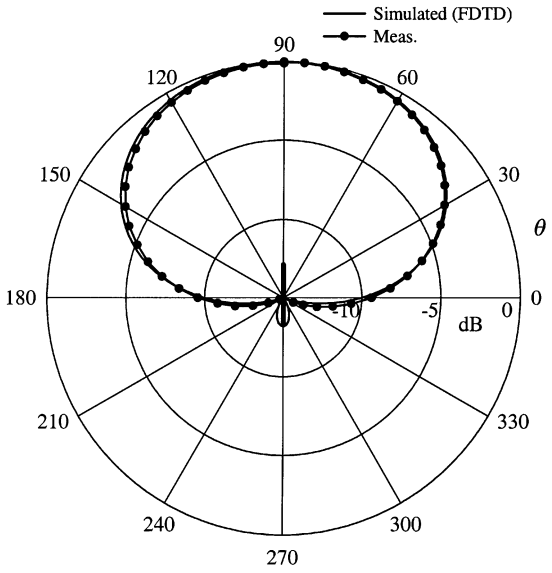

Fig. 7. Comparison of simulated results with measurements for a narrow-band, unidirectional, end-fire design with wires for closed switches. Horizontal field pattern at the center frequency $f = 1.05$ GHz. Both patterns are normalized to 0 dB.

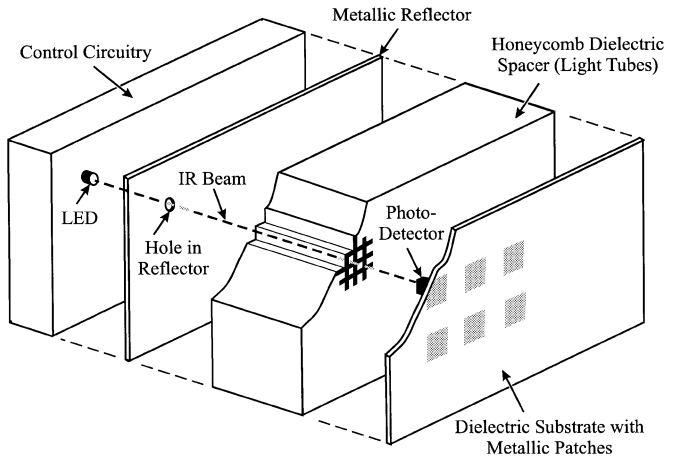

Fig. 8. Schematic drawing showing the arrangement of the major components that make up the prototype RECAP antenna. Details are given for the control of a single switch.

above, one might expect to see strings of patches connected together by closed switches to form linear elements, and these elements to be arranged roughly as in a conventional array, e.g., driven element, reflector, and director; however, as seen in Fig. 3(b), this is not the case. In general, there is no simple discernable relationship between the states of the switches and the goal. This is partly due to the fact that the algorithm must make connections to compensate for the scattering from the unconnected patches. It is clear, however, that the connections near the feed point are often made in a manner to improve the match of the antenna to the transmission line.

The cases described above, along with several other cases not presented, show that switch configurations for the RECAP antenna can be found that allow the antenna to adjust to meet the requirements of different systems. Results from these cases also show that the FDTD simulation is an accurate tool for use in the design procedure. However, for the RECAP antenna to be practical, a switch must be developed that can be electronically controlled, and the control mechanism must not interfere with the electromagnetic performance of the antenna. Such a switch/control system was developed and is described in the next section of this paper.

III. The Prototype RECAP Antenna

The switches and the accompanying control system are an integral part of the RECAP antenna. In the prototype antenna, the switches were electronic and the control was via infrared illumination. Fig. 8 is a schematic drawing showing the overall arrangement of the major components of the prototype antenna. For this antenna, the dielectric substrate containing the metallic patches is FR4 (Nelco 4000-13) with the following measured electrical properties: $\varepsilon_r' = 4.62, \varepsilon_r'' = 0.05, \mu = \mu_o$.[4] A metallic reflector is incorporated into the design. For most of the cases tested, the reflector is the same size as the dielectric substrate containing the metallic patches and spaced 6 cm behind it. The reflector serves two purposes: It makes the

[4]FDTD simulations were performed to determine the effect of the loss in the substate on the antenna performance. For the frequencies used, $f < 2$ GHz, the loss in the substarte was found to be insignificant; it decreased the gain by about 0.1 dB.

antenna practically unidirectional, as opposed to bidirectional, as in Fig. 5, and it isolates the control circuitry from the rest of the antenna. A honeycomb dielectric spacer is placed between the reflector and the dielectric substrate containing the metallic patches. This spacer was fabricated using stereolithography and Vantico SL7510 ($\varepsilon_r' = 3.0, \varepsilon_r'' = 0.10, \mu = \mu_o$). It is about 83% air by volume, and the average electrical properties for the spacer are roughly $\varepsilon_r' = 1.3, \varepsilon_r'' = 0.017, \mu = \mu_o$.

Fig. 8 shows the control path for a single electronic switch. A light-emitting diode (LED, Fairchild QEB421) in the control circuitry sends infrared radiation (peak at 880 nm) through a hole in the reflector. The beam then passes through a channel (light tube) in the honeycomb spacer. The sides of the channel are painted to make them reflective and opaque; this increases the efficiency of light transfer and prevents crosstalk between channels. The light beam finally strikes a photodetector (Fairchild QSB320) located on the backside of the dielectric substrate containing the metallic patches. Here, the light beam activates an electronic switch connecting two patches—when the light is on the switch is closed, and when the light is off the switch is open.

In operation, switch configurations for various goals are first determined using the approach described earlier—FDTD analysis with genetic optimization. These switch configurations are then stored in the memory of the control system and applied as needed. For the prototype RECAP antenna, it takes less than 100 μs to change a switch configuration.

The details for the electronic switches associated with a typical metallic patch (one not at an edge of the board) are given in Figs. 9 and 10. Fig. 9 shows the layout of the components on the front side (side with metallic patch) and back side of the dielectric substrate (circuit board), and Fig. 10 is a circuit diagram for the switch. The circuits on the two sides of the board are connected by the vias marked a, b, and c, in Fig. 9. Note that Fig. 9(a) and (b) are both drawn from the same perspective so that the vias will align.

The four connections to the surrounding patches are on the front side of the board [Fig. 9(a)]. Each connection contains a blocking capacitor ($C = 47$ pF) and a depletion-type FET (Agilent ATF-34143 PHEMT) [20]. Note that two capacitors and two FETs are associated with a typical patch. The rest of the circuitry is on the backside of the board behind the patch [Fig. 9(b)]. This consists of a voltage reference (VR, ZETEX ZXRE125, 1.22 V), two photodetectors (PD), and five resistors ($R = 8.2\,\mathrm{k}\Omega$). The dc bias for the circuit is supplied through resistive lines (8 kΩ/cm, formed from 100 Ω per square Omega-Ply foil) that are also on the backside of the board [Fig. 9(b)]. Resistive lines are used to reduce any scattering from the lines that might distort the field pattern of the antenna. In the bias circuit, the patches in each column of the array are connected in series, and the columns are then connected in parallel. A voltage of about 65 V placed across the bias circuit is sufficient to produce 1.22 V across each of the voltage references.

Referring to the circuit diagram in Fig. 10, the operation of a switch is as follows. When the PD is not illuminated, the impedance of the photodetector is large, and the full voltage of the reference (VR) is between the gate and the source of the depletion-type FET, $v_{\mathrm{GS}} \approx -1.2$ V. The impedance between

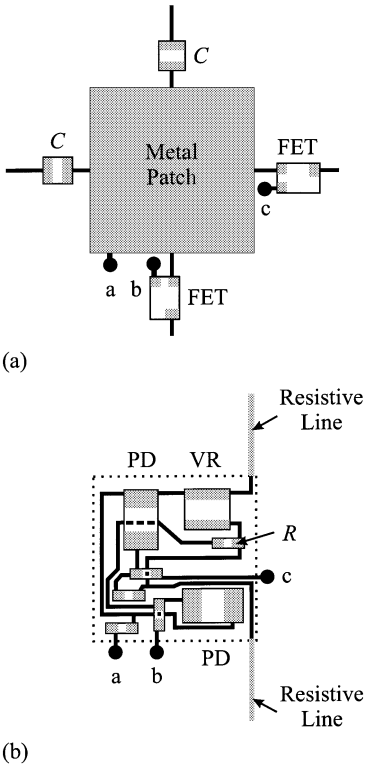

Fig. 9. Schematic drawing showing the layout of the components forming the electronic switches for a typical metallic patch: (a) front side of dielectric substate and (b) back side of dielectric substate. PD—photodetector, VR—voltage reference, FET—transistor, R—resistor (8.2 kΩ), C—capacitor (47 pF).

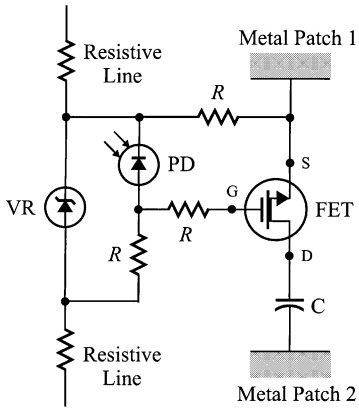

Fig. 10. Circuit diagram for the FET-based electronic switch. PD—photodetector, VR—voltage reference, FET—transistor, R—resistor (8.2 kΩ), C—capacitor (47 pF).

the source and drain of the FET is then high, and the switch is effectively open. When the photodetector is illuminated, the current through the photodetector produces a voltage of about 1 V across the series resistor. The voltage across the photodetector and between the gate and the source of the FET is then $v_{\mathrm{GS}} \approx -0.2$ V. The impedance between the source and drain of the FET is then low, and the switch is effectively closed.

The FET-based switch described above is far from perfect, particularly when operated at microwave frequencies. Therefore, in the FDTD simulations for the prototype RECAP antenna, the switches could not be considered as simple closed

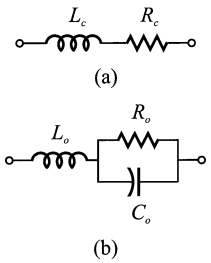

Fig. 11. High-frequency, small-signal equivalent circuits for the FET. (a) Closed state: $R_c = 4.3\,\Omega, L_c = 2.6$ nH. (b) Open state: $R_o = 5.9$ k$\Omega, L_o = L_c = 2.6$ nH, $C_o = 0.49$ pF.

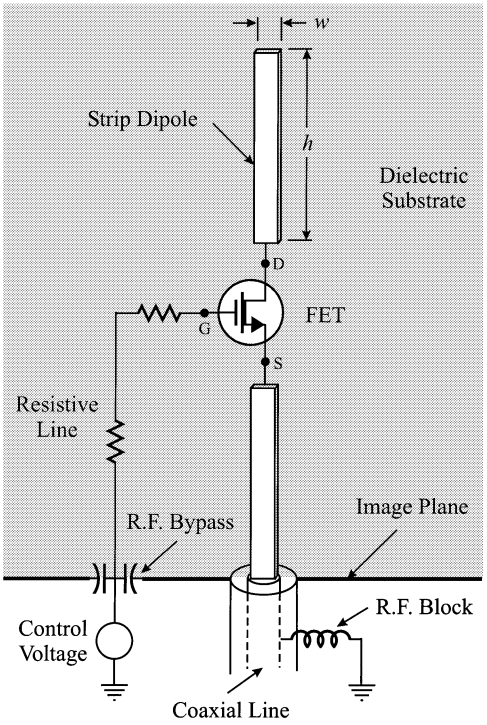

Fig. 12. Schematic drawing for the experimental fixture used to measure the high-frequency, small-signal equivalent circuit parameters of the FET.

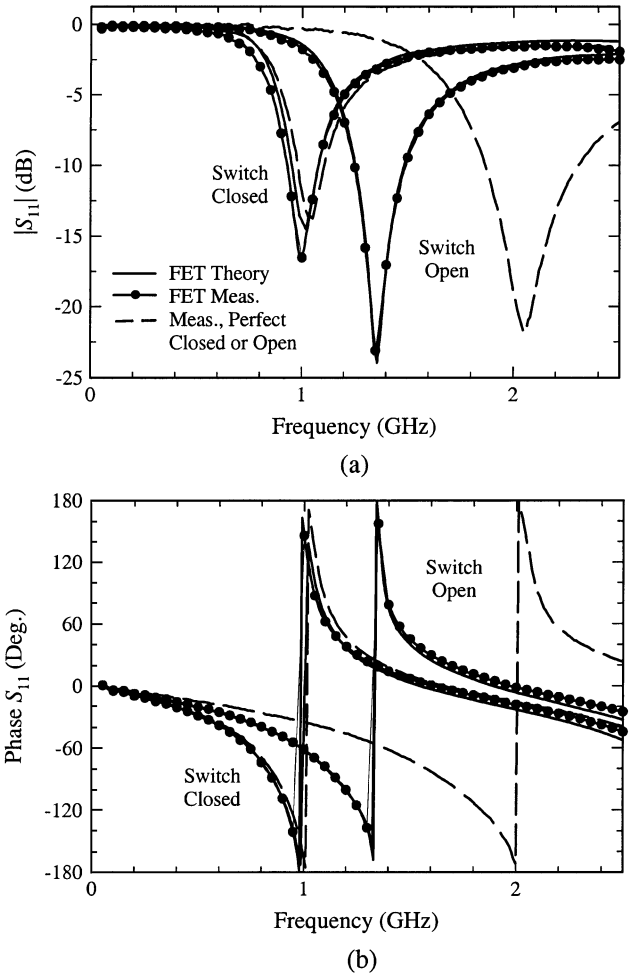

Fig. 13. Results for S_{11} of the monopole antenna that were used in determining the high-frequency, small-signal equivalent circuit parameters for the FET. (a) Amplitude and (b) phase.

or open connections, as done earlier in Section II. A suitable model had to be developed for incorporating the properties of the switch in the FDTD analysis. For this work, the FET was represented by the high-frequency, small-signal equivalent circuits shown in Fig. 11. In the closed state [Fig. 11(a)], the circuit is a resistor R_c in series with an inductor L_c, and in the open state [Fig. 11(b)], the circuit is an inductor $L_o = L_c$ in series with the parallel combination of a resistor R_o and a capacitor C_o.

To determine values for the circuit elements in the model, the FET was placed in the fixture shown in Fig. 12. The fixture creates an environment for the FET that is similar to that in the RECAP antenna, i.e., the FET is placed uncovered in a radiating structure, rather than in a traditional closed fixture, such as a coaxial line. The FET is at the center of a strip monopole ($h = 3$ cm, $w = 2$ mm) that is fed at its lower end through an image plane by a coaxial line. The length of the monopole was chosen so that resonance occurs within the bandwidth of interest. This increases the sensitivity of the measurement to the state of the switch (open or closed). The control voltage is applied to the gate of the FET through a resistive line (formed from 100 Ω per square Omega-Ply foil) that has a total resistance of about 10.5 kΩ.

An FDTD model was constructed for the fixture shown in Fig. 12. The model included the equivalent circuits for the FET, shown in Fig. 11, as well as the dielectric substrate and resistive line. Calculations of the reflection coefficient S_{11} at the end of the coaxial line attached to the antenna were compared with measurements, and the values of the circuit elements that gave the best agreement were determined using a simple optimizer ($R_c = 4.3\,\Omega, L_c = L_o = 2.6$ nH, $R_o = 5.9\,\text{k}\Omega, C_o = 0.49$ pF). Fig. 13 shows the magnitude and the phase of the reflection coefficient S_{11} versus frequency. The results from the FDTD simulation (switch open and switch closed) are the solid lines, and those from the measurements are the lines with solid dots. The two results are seen to agree fairly well over the range of frequencies for the RECAP antenna $f < 2$ GHz. For reference, measured results for a "perfect open" and a perfect closed" are shown as dashed lines. The perfect open was obtained by simply removing the FET from the fixture, and the perfect closed was obtained by replacing the FET in the fixture by a metal strip. The need for the circuit model for the FET is evident, particularly

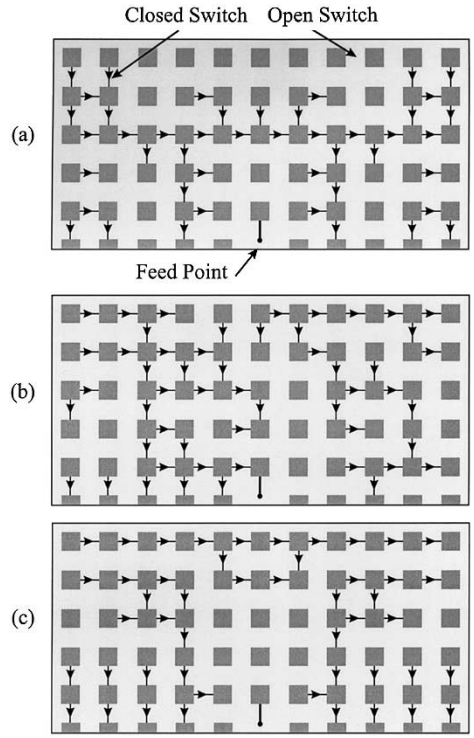

Fig. 14. Schematic drawings for the RECAP antenna (monopole form) showing which FET switches are open and closed. (a) Narrow-band broadside design. (b) Narrow-band design steered to $\theta = 45°$. (c) Broadband, broadside design.

when one considers the difference between the results (amplitude and phase) for the perfect open and the open switch. In the open state, the resistance R_o of the FET is large and has little effect, so the capacitor C_o is the most critical element.

IV. Performance of the Prototype RECAP Antenna: Comparison of Theory With Experiment

A full theoretical electromagnetic model was constructed for the prototype RECAP antenna, and FDTD results obtained with this model were used with the genetic algorithm to determine the configurations for the FET-based switches (which ones are open and which ones are closed) that best meet specified goals. The theoretical electromagnetic model included the metallic patches and the dielectric substrate, the reflector with dielectric spacer, and the aforementioned equivalent circuit models for the FET. The theoretical electromagnetic model did not include the other circuit elements associated with the switch, e.g., the elements in the control circuit. These elements are generally not involved in the high-frequency performance of the antenna.

The switch configuration shown in Fig. 14(a) is for a narrow-band, unidirectional, broadside design for the frequency $f = 1.25$ GHz. The goal for this design is that the realized gain of the RECAP antenna should equal or exceed the directivity of a uniform sheet of vertically directed current of the same size placed 6 cm in front of a reflecting plane. This is a rather optimistic goal, because the actual reflector used with the RECAP antenna is of finite size (22.5×22 cm), whereas the reflector for the goal is infinite in size. Fig. 15(a) shows the realized gain

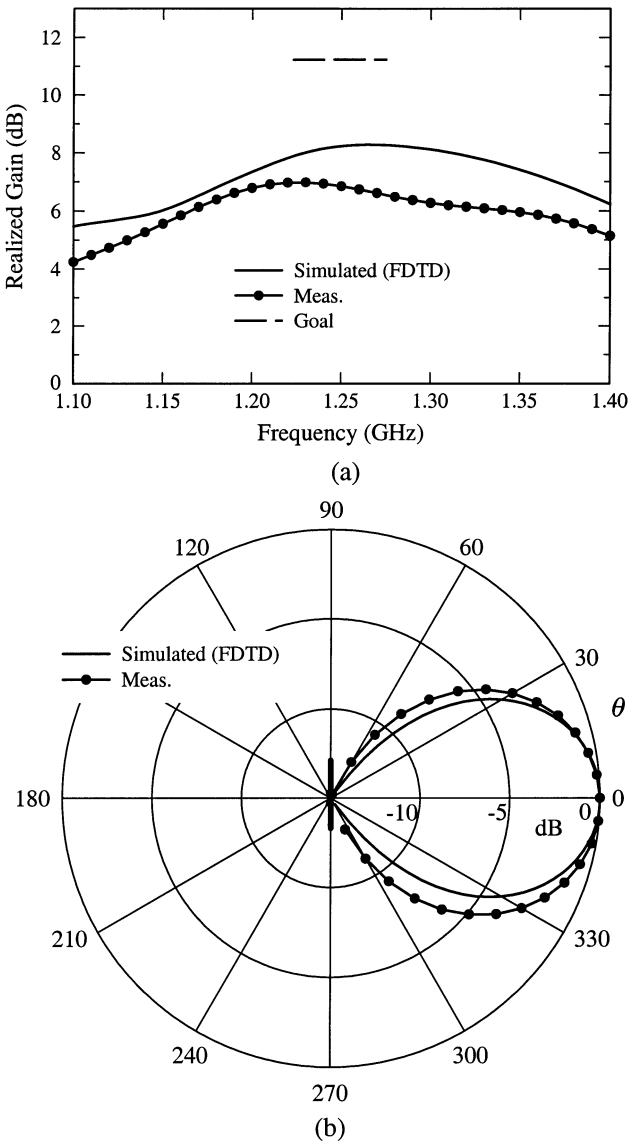

Fig. 15. Comparison of simulated results with measurements for a narrow-band, broadside design with FET-based switches. (a) Realized gain versus frequency. (b) Horizontal field pattern at the center frequency $f = 1.25$ GHz. Both patterns are normalized to 0 dB.

versus frequency, and Fig. 15(b) shows the horizontal field pattern at the design frequency. In these graphs, the dashed line is the aforementioned goal, the solid line is the FDTD simulation, and the line with the solid dots is the measured result. At the frequency for the design, the simulated and measured realized gains differ by about only 1.2 dB. The realized gain for the design, however, is about 3 dB below the goal. This is considerably larger than the difference between the design and goal observed earlier, Figs. 4 and 6, when wires were used for closed switches. Part of this difference can be attributed to the loss of energy in the switches, and it will be discussed in detail later in this paper. The simulated and measured field patterns, shown in Fig. 14(b), are in good agreement.

The switch configuration shown in Fig. 14(b) is also for a design at the frequency $f = 1.25$ GHz, only now the main beam of the antenna is to be at $\theta = 45°$, as opposed to broadside. The goal is again that the realized gain of the RECAP antenna should

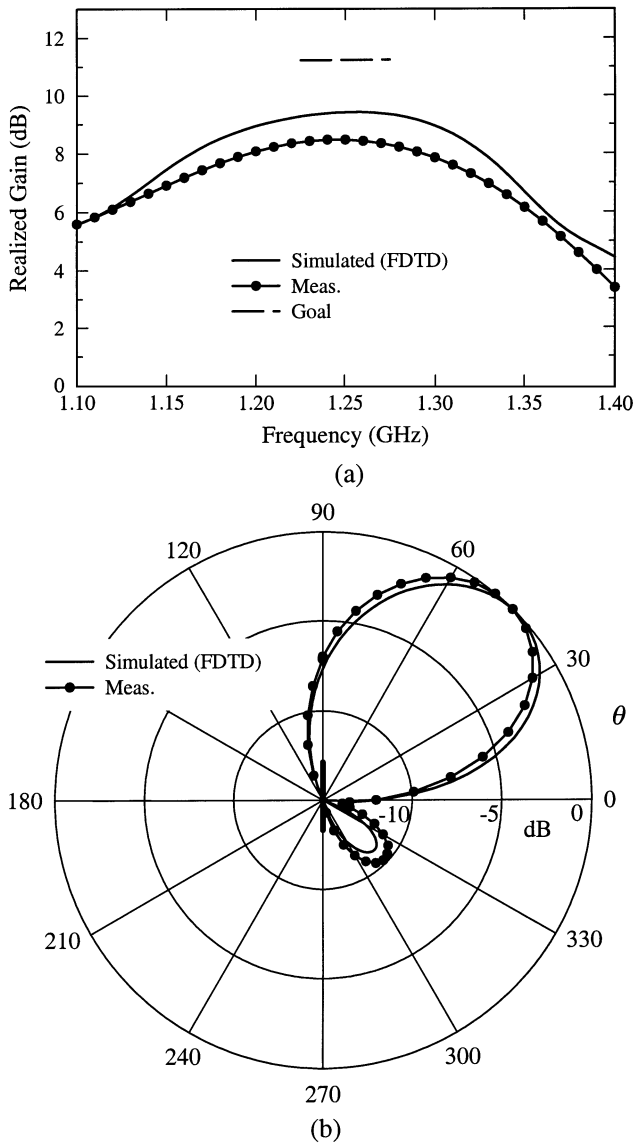

Fig. 16. Comparison of simulated results with measurements for a narrowband design steered to $\theta = 45^\circ$ with FET-based switches. (a) Realized gain versus frequency. (b) Horizontal field pattern at the center frequency $f = 1.25$ GHz. Both patterns are normalized to 0 dB.

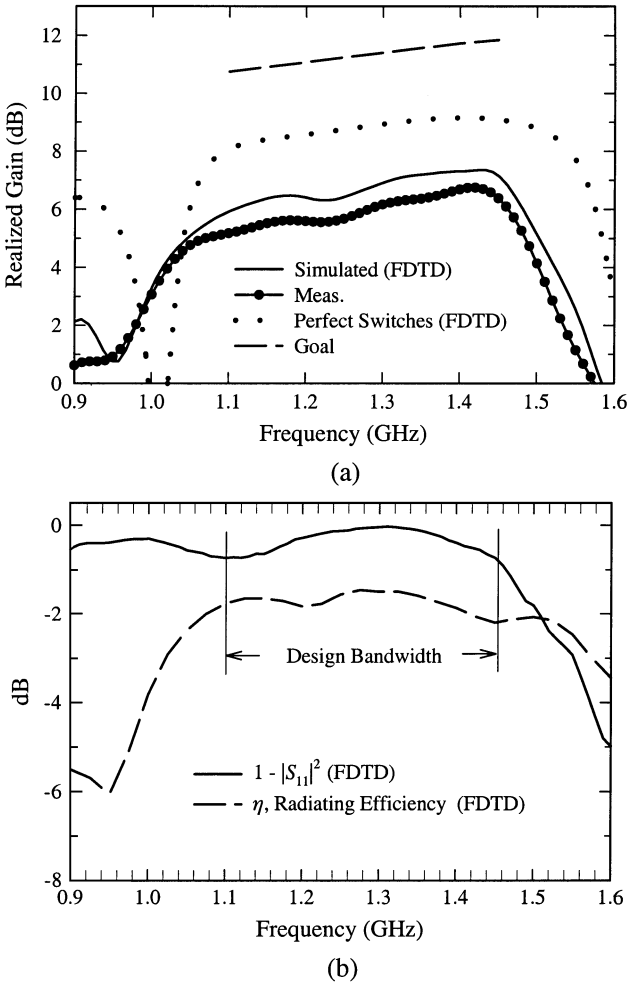

Fig. 17. Results for a broadband, broadside design with FET-based switches. (a) Realized gain versus frequency, simulation, and measurement. (b) Factors that determine the energy lost: $1-|S_{11}|^2$ and the radiating efficiency η.

equal or exceed the directivity of a uniform sheet of current with an infinitely large planar reflector; only now the current is phased to produce a beam at $\theta = 45^\circ$. There is one physical difference between this antenna and the one described earlier: The metallic reflector is 47×52 cm rather than 22.5×22 cm. At the frequency for the design, the simulated and measured realized gains, shown in Fig. 16(a), differ by about only 1.0 dB, and the realized gain for the design is about 2 dB below the goal. The shapes of the simulated and measured field patterns, shown in Fig. 16(b), are nearly the same, and both peak near the angle $\theta = 45^\circ$. These two examples clearly show that the main beam for the prototype RECAP antenna can be steered by changing the switch configuration.

The switch configuration shown in Fig. 14(c) is for a broadband, unidirectional, broadside design for the frequency range $1.10\ \text{GHz} \leq f \leq 1.45$ GHz (bandwidth of 27%). Fig. 17(a) shows the realized gain versus frequency, and Fig. 18 shows the horizontal field pattern at three frequencies within the design bandwidth: $f = 1.10, 1.27$, and 1.45 GHz. The goal (dashed line) is that the realized gain of the RECAP antenna should equal or exceed the directivity of a uniform sheet of vertically directed current of the same size with an infinitely large planar reflector. There is generally good agreement between the simulated results (solid lines) and the measured results (lines with solid dots). The realized gains shown in Fig. 17(a) differ by less than 1.0 dB, and the field patterns shown in Fig. 18 are nearly identical. However, the realized gain for the design is about 4 dB below the goal. While the goal is rather optimistic (the directivity of a uniform current sheet with an infinitely large planar reflector), the results presented in Section II, where wires were used for closed switches, suggest that this difference could be smaller.

The FDTD simulation for the RECAP antenna was used to examine the above-mentioned difference between the goal and the achieved results for the realized gain of the broadband, unidirectional, broadside design, shown in Fig. 14(c). Two factors can cause a loss of energy and a resultant decrease in the realized gain of the antenna: 1) mismatch of the input impedance of the antenna to the characteristic impedance of the feeding transmission line, which reduces the radiated power by the factor

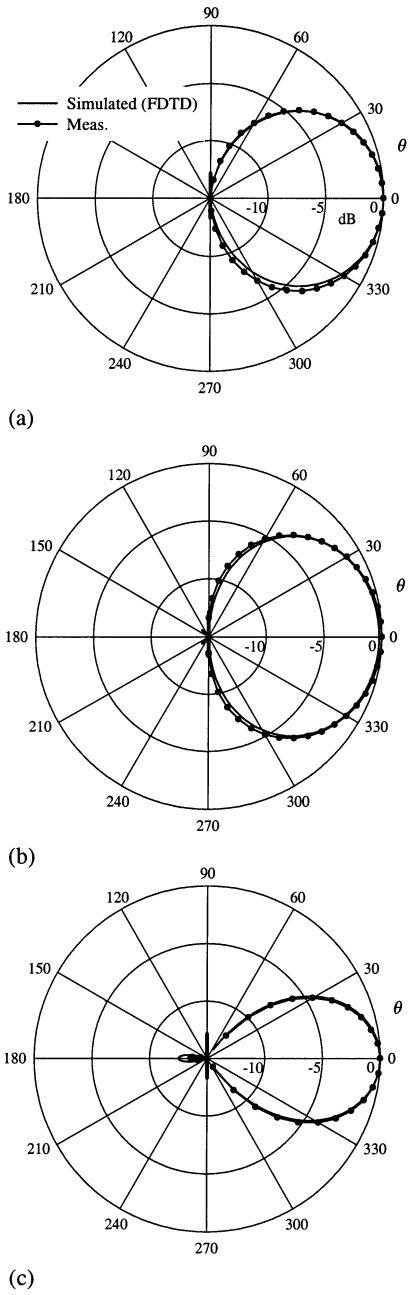

Fig. 18. Horizontal field patterns for a broadband, broadside design with FET-based switches. (a) $f = 1.1$ GHz, (b) $f = 1.27$ GHz, (c) $f = 1.45$ GHz. All patterns are normalized to 0 dB.

$(1 - |S_{11}|^2)$, and 2) dissipation in the components of the antenna, which reduces the radiated power by the factor η, the radiating efficiency. In Fig. 17(b) both of these quantities are plotted versus frequency. The loss due to mismatch is less than 20% (−0.7 dB) over the design bandwidth, while the loss due to dissipation is roughly 37% (−2 dB) over the entire design bandwidth. Thus, the dissipation in the components of the antenna is the dominant loss mechanism for this design. Additional calculations show that the energy dissipated in the substrate and dielectric spacer is practically negligible, so most of the loss is associated with the finite resistance of the switches in the closed state $(R_c = 4.3\,\Omega)$.

An important question for the future development of the RECAP antenna is—How close would the realized gain of the antenna be to the goal if the switches had no loss? Notice that this question cannot be answered by simply setting the resistance of the closed switches to zero in the present switch configuration [Fig. 14(c)], because this switch configuration is the result of an optimization in which the resistance of the switches was taken into account. To answer this question, the optimization was re-run assuming lossless switches (wires for the closed switches and gaps for the open switches, as in Section II). The results of that optimization are shown as a dotted line in Fig. 17(a). Now the realized gain is about 2.3 dB below the goal, as opposed to 4 dB below with the FET-based switches. The possibility of obtaining switches that can approach this level of performance will be discussed in the next section.

V. Alternative Switch/Control Strategies

The method described in Section III for controlling the switches in the RECAP antenna (optical control using LEDs and photodetectors) is only one of a number of approaches that were developed and tried. Here we will present a brief description of some of the other approaches, emphasizing the positive and negative aspects of each. Additional details for these approaches are given in [15].

All of these approaches can be grouped into two categories. The first category includes those approaches for which the logic for switch control is located on the aperture surface. For these approaches, the logic chips on the aperture receive a digital signal identifying the desired configuration. The chips then activate the appropriate switches to set this configuration. The motivation for putting the logic on the aperture surface is to remove the requirement of a fixed image plane integrated into the antenna. This allows a single aperture surface to be easily placed into antenna implementations with different image plane spacings, or to be operated with no image plane at all, depending on the application at hand.

The second category includes those approaches for which the logic for switch control is separated from the aperture. The prototype RECAP antenna, described in Section III, is an example from this category. Here, the decision as to which switches are to be activated is made in the control circuitry located behind the image plane.

For all of the approaches to be described, FET-based switches were used, and they were essentially the same as the one described in Section III.

A. Control With Logic on the Aperture Surface

Two strategies were used to communicate the digital signal to the logic chips on the aperture surface. For both of these strategies, there is one logic chip mounted on the board per metallic patch, and each logic chip controls two switches (except at the edges of the aperture). The first strategy employs resistive lines on the aperture surface to carry the digital signal to the logic chips and power the switches. These lines are identical in construction to those used with the approach described in Section III. Tests of this strategy revealed a performance tradeoff between the deterioration of the antenna performance due to scattering from the lines (also loss in the lines) and the speed

TABLE I
COMPARISON OF VARIOUS STRATEGIES FOR CONTROLLING THE SWITCHES

Strategy	Resistive Loss	Time to Switch Configuration	Bias Voltage	Accuracy of FDTD Simulation	Complexity of Interface
Resistive Lines	Significant	240μsec	< 5 Volts	Good	Moderate
Inductive Coupling	Negligible	Not Tested	Arbitrary	Poor	Low
Photo-Detector*	Negligible	20μsec	Arbitrary	Good	Highest
Solar Cell	Negligible	100μsec	0.6 Volts	Good	High

*The results for the photo-detector strategy are for the second-generation design, not for the prototype RECAP antenna.

at which a configuration could be changed. Increasing the resistance per unit length of the lines reduced the scattering from the lines; however, it also increased the time constant for transmitting a digital signal over the lines to the logic chips. Thus, satisfactory performance of the antenna required highly resistive lines and appreciable times for changing configurations.

The second strategy used to communicate with the logic chips on the aperture surface employs inductive coupling. Here, a low-frequency RF carrier (13.5 MHz) is modulated with the digital signal and used to both control and power the switches. This signal is radiated by a rectangular, two-turn loop surrounding the aperture, and it is received by small, 20-turn coils on the aperture surface. These coils replace the metallic patches shown in Fig. 1 and are designed to serve as both a coupling element and an antenna element. Notice that this strategy eliminates all physical contact with the aperture surface other than the connection at the feed point.

For this strategy, it was impractical to use the FDTD method with the genetic algorithm to optimize the antenna. The necessary accuracy from the FDTD simulation required that all of the 20-turn coils on the aperture surface be modeled. This resulted in extremely small cell size and impractical requirements for computer memory and run time. In order to overcome this limitation, a new optimization procedure was developed in which calculations of the realized gain using the FDTD method were replaced by direct measurements of the realized gain in the experimental setup shown in Fig. 2. The antennas designed using the new procedure had reasonable performance for frequencies in the range 0.9–1.25 GHz.

B. Control With Logic Removed From the Aperture Surface

Two strategies were tested in which the logic for switch control was separated from the aperture. Both of these strategies utilized optical coupling. The first strategy used light-emitting diodes and photodetectors and resulted in the prototype RECAP antenna described in Section III. The second strategy used light-emitting diodes with solar cells and will be described now.

The arrangement of the components is essentially the same as shown in Fig. 8 with the photodetectors replaced by solar cells. The radiation from the LEDs is modulated with the digital signal and used to both control and power the switches. Note that this strategy is different from the one that used photodetectors, because it does not require resistive lines to supply bias to the FETs. This strategy eliminates all physical contact with the aperture surface other than the connection at the feed point, as did the strategy utilizing inductive coupling described earlier.

For this strategy, we were limited by the voltage output (about 0.6 V) of the commercially available solar cells of the required size (two solar cells must fit behind a single 1×1 cm metallic patch). This limitation is important because the bias voltage for the FET can limit the RF power handling of the switches. Note that a customized solar cell that is designed for high voltage output (low current) would allow for higher bias voltages. There was an additional problem with this strategy: The speed for switching is limited by the voltage decay of the solar cell once the illumination to the cell is turned off. For the particular circuit used, this speed was considerably slower than obtained with the strategy employing photodetectors. Apart from these limitations, the antennas designed using this strategy had reasonable performance for frequencies in the range 0.9–1.45 GHz.

Table I lists the advantages and disadvantages for all of the strategies that were investigated. Note that the "resistive loss" mentioned in the table is the loss due to dissipation of energy in the control system. All of these strategies employ FET switches and thus are subject to the energy dissipation in the FET.

C. The Potential for MEMS-Based Switches

As shown in the previous section, the FET-based switches used in the prototype antenna have inherent loss that reduces the radiating efficiency of the antenna. The use of the FET also introduces a limitation on the power that can be handled by the antenna and the possibility of unwanted nonlinear effects both on transmission and reception. It would be highly desirable to have a switch for the RECAP antenna that alleviates these potential problems. A MEMS switch offers promise in this regard. Unfortunately, during the time the RECAP antenna was being developed, a suitable RF microwave MEMS switch was not available, and this is still the case. MEMS technology is in a state of rapid development, and, undoubtedly, a suitable switch will one day be available. When it is, the RECAP antenna could serve as a practical testbed for the switch.

VI. SUMMARY AND CONCLUSION

A reconfigurable aperture antenna was developed. This is a planar array of electrically small, metallic patches that are interconnected by switches. The antenna is reconfigured to meet different performance goals by changing the switches that

are open and closed. The switch configuration for a particular goal is determined through optimization using the genetic algorithm. The basic concept for this RECAP antenna was verified by comparing theoretical results with measurements for designs in which the switches were simply wires connecting the patches. A prototype for the RECAP antenna was designed and built. In the prototype, FET-based electronic switches were used with optical control. Theoretical results for the prototype antenna were in good agreement with measurements for cases in which electronic reconfiguration was used to change the bandwidth of operation or steer the pattern of the antenna. These results demonstrate the potential of this RECAP antenna for practical applications.

After the prototype RECAP antenna discussed in this paper was built and tested, a second-generation FET-based switch was designed and employed in a RECAP antenna built for a specific application. The new switch has better performance than the prototype because of three major modifications. First, the new switch uses an unpackaged FET that is connected to the circuit with wire bonds, whereas the old switch used a packaged FET. This modification reduces the open-state capacitance of the switch to 0.26 pF, which permits operation to higher frequencies. Second, the bias voltages for the open and closed states were extended to $v_{\rm GS} \approx -8.2$ and 0 V, respectively. This modification allows the switch to handle higher RF power. Third, a comparator was incorporated to actively drive the bias voltage to the open or closed value. This modification allows the switch to change state in a shorter time and also improves the sensitivity of the optical link. The RECAP antenna that uses this new switch operates to a frequency of 2.5 GHz, handles about 1 W of RF power, and switches state in a time of approximately 20 μs.

The new FET-based switch, however, does not overcome the limitation on radiating efficiency imposed by the resistance of the switch in the closed state. The energy lost in the switches reduces the radiating efficiency of the antenna to a point where it might be unacceptable for some applications. The use of a MEMS based switch would, most likely, alleviate this problem. Thus, this RECAP antenna could serve as a practical testbed for an RF microwave MEMS switch.

ACKNOWLEDGMENT

The authors would like to thank Dr. J. G. Maloney, Dr. M. P. Kesler, and Dr. L. M. Lust for their help at the early stage of this work.

REFERENCES

[1] K. C. Gupta, J. Li, R. Ramadoss, C. Wang, Y. C. Lee, and V. M. Bright, "Design of frequency-reconfigurable rectangular slot ring antennas," in *IEEE Antennas and Propagation Int. Symp.*, Salt Lake City, UT, July 2000. CD-ROM.

[2] J. H. Schaffner, R. Y. Loo, D. F. Sevenpiper, F. A. Dolezal, G. L. Tangonan, J. S. Colburn, J. J. Lynch, J. J. Lee, S. W. Livingston, R. J. Broas, and M. Wu, "Reconfigurable aperture using RF MEMS switches for muti-octave tunability and beam steering," in *IEEE Antennas and Propagation Int. Symp.*, Salt Lake City, UT, July 2000. CD-ROM.

[3] F. Yang and Y. Rahmat-Samii, "Patch antennas with switchable slots (PASS): Concept, theory and applications," in *Proc. Antenna Applications Symp.*. Monticello, IL, Sept. 2001, pp. 84–103.

[4] D. Peroulis, K. Sarabandi, and L.P.B. Katehi, "A planar VHF reconfigurable slot antenna," in *IEEE Antennas and Propagation Int. Symp.*, Salt Lake City, UT, July 2001. CD-ROM.

[5] B. T. Perry, C. M. Coleman, B. F. Basch, E. J. Rothwell, and J. E. Ross, "Self-structuring antenna for television reception," in *IEEE Antennas and Propagation Int. Symp.*, Salt Lake City, UT, July 2001. CD-ROM.

[6] W. H. Weedon, W. J. Payne, and G. M. Rebeiz, "MEMS-switched reconfigurable antennas," in *IEEE Antennas and Propagation Int. Symp.*, Salt Lake City, UT, July 2001. CD-ROM.

[7] M. A. Ali and P. Wahid, "A reconfigurable Yagi array for wireless applications," in *IEEE Antennas and Propagation Int. Symp.*, San Antonio, TX, June 2002. CD-ROM.

[8] J. Hazen, R. Clark, P. Mayes, and J. T. Bernhard, "Stacked reconfigurable antennas for space-based radar applications," in *Proc. Antenna Applications Symp.*. Monticello, IL, Sept. 2001, pp. 59–69.

[9] J. C. Veihl, R. E. Hodges, D. McGrath, and C. Monson, "Reconfigurable aperture decade bandwidth array," in *IEEE Antennas and Propagation Int. Symp.*, Salt Lake City, UT, July 2000. CD-ROM.

[10] V. C. Sanchez, W. E. McKenzie, III, and R. E. Diaz, "Broadband antennas over electronically reconfigurable artificial magnetic conductor surfaces," in *Proc. Antenna Applications Symp.*. Monticello, IL, Sept. 2001, pp. 70–83.

[11] D. Sievenpiper, J. Schaffner, B. Loo, G. Tangonan, R. Harold, J. Pikulski, and R. Garcia, "Electronic beam steering using a varactor-tuned impedance surface," in *IEEE Antennas and Propagation Int. Symp.*, Salt Lake City, UT, July 2001. CD-ROM.

[12] A. Fathy, A. Rosen, F. McGinty, G. Taylor, S. Perlow, and M. ElSherbiny, "Silicon based reconfigurable antennas," in *IEEE Antennas Propagation Int. Symp.*, Salt Lake City, UT, July 2000. CD-ROM.

[13] J. G. Maloney, M. P. Kesler, P. H. Harms, and G. S. Smith, "Fragmented aperture antennas and broadband antenna ground planes,", U.S. Patent 6 323 809 B1, Nov. 27, 2001.

[14] J. G. Maloney, M. P. Kesler, L. M. Lust, L. N. Pringle, T. L. Fountain, P. H. Harms, and G. S. Smith, "Switched fragmented aperture antennas," in *Proc. IEEE Antennas Propagation Int. Symp.*, Salt Lake City, UT, July 2000. CD-ROM.

[15] L. N. Pringle, P. Friederich, L. Fountain, P. Harms, D. Denison, E. Kuster, S. Blalock, R. Prado, G. Kiesel, G. Smith, M. Allen, K. Kim, J. Maloney, and M. Kesler, "Architecture and performance of a reconfigurable aperture," in *Proc. Antenna Applications Symp.*. Monticello, IL, Sept. 2001, pp. 36–58.

[16] L. N. Pringle, P. G. Friederich, S. P. Blalock, G. N. Kiesel, P. H. Harms, D. R. Denison, E. Kuster, T. L. Fountain, and G. S. Smith, "GTRI reconfigurable aperture design," in *IEEE Antennas Propagation Int. Symp.*, San Antonio, TX, June 2002. CD-ROM.

[17] *IEEE Standard Test Procedures for Antennas*, Antenna Standards Committee, IEEE Antennas and Propagation Society, 1979.

[18] J. G. Maloney and G. S. Smith, "Modeling of antennas," in *Advances in Computational Electrodynamics: The Finite-Difference Time-Domain Method*, A. Taflove, Ed. Boston, MA: Artech House, 1998, ch. 7.

[19] D. L. Carroll, FORTRAN genetic algorithm front-end driver.

[20] *Technical Data: Low Noise Pseudomorphic HEMT in Surface Mount Plastic Package*, 2000.

Lon N. Pringle received the B.E.E. degree from the Georgia Institute of Technology (Georgia Tech), Atlanta, in 1979 and the Ph.D. degree in theoretical physics from the University of South Carolina, Columbia, in 1988.

Since 1988, he has served as a Research Scientist in the Signature Technology Laboratory, Georgia Tech Research Institute (GTRI), where he is now a Principle Research Scientist. During this time his research has encompassed aperture surface design, infrared and optical scattering surface design, scattering processes within paints and binders, and numerical simulation of scattering processes.

Paul H. Harms (S'80–M'92) received the Ph.D. degree in electrical engineering from the University of Illinois at Urbana Champaign, in 1992.

He is currently with the Georgia Tech Research Institute (GTRI), Atlanta, as a Research Engineer in electromagnetics. His interests include computational methods, antenna design and optimization with genetic algorithms, and antenna measurements. He also has experience in modeling frequency selective surfaces, scattering from underwater objects, radio-frequency heating of objects, and electronic packaging and connectors for high speed digital circuits.

Stephen P. Blalock received the bachelor's and master's degrees in electrical engineering technology from Southern Polytechnic State University, Marietta, GA, in 1994 and 1998, respectively.

Since 1995, he has been with the Georgia Tech Research Institute (GTRI), Atlanta, where since 1998 he has supervised all measurement facilities for the Signature Technology Laboratory. His experience in RF measurement systems encompasses focused beam measurements, low frequency scanning, reflection plane measurements, and compact range measurements.

Gregory N. Kiesel received the B.E.E. and M.S.E.E. degrees from Georgia Institute of Technology (Georgia Tech), Atlanta, in 1999 and 2003, respectively.

From 1999 to 2001, he was a Design Engineer for Raytheon Systems in Saint Petersburg, FL. In 2001, he joined the Faculty of the Georgia Tech Research Institute (GTRI), Atlanta, as a Research Engineer. His technical interests include antenna design, balun design, analog circuit design, and signal processing of electromagnetic signals.

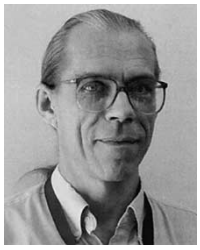

Eric J. Kuster received the B.S. degree in mathematics from Saint Lawrence University, Canton, NY, in 1972 and the M.S. and Ph.D. degrees in physics from Georgia Institute of Technology (Georgia Tech), Atlanta, in 1973 and 1983, respectively.

From 1983 to 1984, he was a Postdoctoral Research Fellow at Georgia Tech. In 1984, he joined the Georgia Tech Research Institute (GTRI), Atlanta, where he is currently a Principal Research Scientist. His technical interests include numerical modeling of electromagnetic propagation in frequency selective surfaces and artificial dielectrics, RCS modeling and measurement, and antenna design.

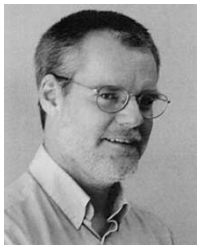

Paul G. Friederich (M'78) received the B.S. degree in biomedical engineering from Vanderbilt University, Nashville, TN, in 1979 and the M.S. degree in electrical engineering from the Georgia Institute of Technology (Georgia Tech), Atlanta, in 1983.

Since 1980, he has been with the Georgia Tech Research Institute (GTRI), Atlanta. He has contributed to research efforts to develop methods to characterize electromagnetic properties of materials and to characterize antenna performance and scattering characteristics. Since 2000, he has been the Technical Director of the Electromagnetic Apertures and Scattering Group, Signature Technology Laboratory, GTRI. His technical interests include design and physical limitations of wide-band antennas, low-scattering antennas, and laboratory characterization of scattering and radiation problems from RF to millimeter wavelengths.

Mr. Friederich is a Member of Tau Beta Pi.

Ronald J. Prado (M'87) received the bachelor's and M.S. degrees from the Georgia Institute of Technology (Georgia Tech), Atlanta, in 1987 and 1992, respectively, both in electrical engineering.

He is a Senior Research Engineer in the Electronic Systems Laboratory, Georgia Tech Research Institute. His technical interests include data acquisition and control system design and embedded system design and development.

Mr. Prado is a Member of ITEA and AOC.

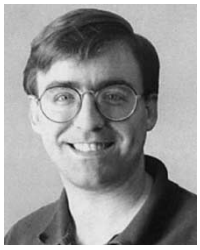

John M. Morris received the B.E.E. and M.S.E.E. degrees from Georgia Institute of Technology (Georgia Tech), Atlanta, in 1989 and 1990, respectively.

From 1990 to 1995, he worked in a microprocessor design group for Motorola Semiconductor Product Sector, Austin, TX. In 1995, he joined the Georgia Tech Research Institute (GTRI), Atlanta, where he is currently a Research Engineer. His technical interests include microprocessor design, logic simulation, behavioral modeling, commercial product realization, and design for testability.

Mr. Morris is a Member of Tau Beta Pi, Eta Kappa Nu, and Phi Kappa Phi.

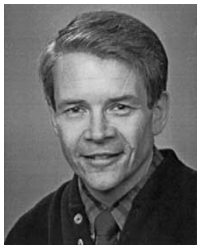

Glenn S. Smith (S'65–M'72–SM'80–F'86) received the B.S.E.E. degree from Tufts University, Medford, MA, in 1967 and the S.M. and Ph.D. degrees in applied physics from Harvard University, Cambridge, MA, in 1968 and 1972, respectively.

From 1972 to 1975, he was a Postdoctoral Research Fellow at Harvard University and a part-time Research Associate and Instructor at Northeastern University, Boston, MA. In 1975, he joined the Faculty of the School of Electrical and Computer Engineering, Georgia Institute of Technology, Atlanta, where he is currently Regents' Professor and John Pippin Chair in Electromagnetics. He is the author of *An Introduction to Classical Electromagnetic Radiation* (Cambridge, U.K.: Cambridge University Press, 1997) and coauthor of *Antennas in Matter: Fundamentals, Theory and Applications* (Cambridge, MA: MIT Press, 1981). He also authored the chapter "Loop Antennas" in *Antenna Engineering Handbook* (New York: McGraw-Hill, 1993. His technical interests include basic electromagnetic theory and measurements, antennas and wave propagation in materials, and the radiation and reception of pulses by antennas.

Prof. Smith is a Member of Tau Beta Pi, Eta Kappa Nu, and Sigma Xi, and the International Scientific Radion Union (URSI) Commissions A and B.